VSP

Advanced Robotics 22 (2008) 657–687

ADVANCED ROBOTICS
www.brill.nl/ar

Full paper

Kinematic Analysis of a Macro–Micro Redundantly Actuated Parallel Manipulator

Hamid D. Taghirad [a,*] **and Meyer Nahon** [b]

[a] Advanced Robotics and Automated Systems, Department of Electrical Engineering, K. N. Toosi University of Technology, PO Box 16315-1355, Tehran

[b] Center for Intelligent Machines, Department of Mechanical Engineering, McGill University, Montréal, Québec H3A 2K6, Canada

Received 6 March 2007; accepted 12 July 2007

Abstract

In this paper the kinematic and Jacobian analysis of a macro–micro parallel manipulator is studied in detail. The manipulator architecture is a simplified planar version adopted from the structure of the Large Adaptive Reflector (LAR), the Canadian design of the next generation of giant radio telescopes. This structure is composed of two parallel and redundantly actuated manipulators at the macro and micro level, which both are cable-driven. Inverse and forward kinematic analysis of this structure is presented in this paper. Furthermore, the Jacobian matrices of the manipulator at the macro and micro level are derived, and a thorough singularity and sensitivity analysis of the system is presented. The kinematic and Jacobian analysis of the macro–micro structure is extremely important to optimally design the geometry and characteristics of the LAR structure. The optimal location of the base and moving platform attachment points in both macro and micro manipulators, singularity avoidance of the system in nominal and extreme maneuvers, and geometries that result in high dexterity measures in the design are among the few characteristics that can be further investigated from the results reported in this paper. Furthermore, the availability of the extra degrees of freedom in a macro–micro structure can result in higher dexterity provided that this redundancy is properly utilized. In this paper, this redundancy is used to generate an optimal trajectory for the macro–micro manipulator, in which the Jacobian matrices derived in this analysis are used in a quadratic programming approach to minimize performance indices like minimal micro manipulator motion or singularity avoidance criterion.

Keywords

Parallel manipulator, inverse kinematics, forward kinematics, Jacobian analysis, singularity, macro–micro robot, redundancy

* To whom correspondence should be addressed. E-mail: taghirad@kntu.ac.ir

 DOI:10.1163/156855308X305263

1. Introduction

An international consortium of radio astronomers and engineers has agreed to investigate technologies to build the Square Kilometer Array (SKA), a centimeter-to-meter wave radio telescope for the next generation of investigation into cosmic phenomena [1, 2]. A looming 'sensitivity barrier' will prevent current telescopes from making much deeper inroads at these wavelengths, particularly in studies of the early universe. The Canadian proposal for the SKA design consists of an array of 30–50 individual antennae whose signals are combined to yield the resolution of a much larger antenna. Each antenna would use the Large Adaptive Reflector (LAR) concept put forward by a group led by the National Research Council of Canada, and supported by university and industry collaborators [3, 4]. The LAR design is applicable to telescopes up to several hundred meters in diameter. However, design and construction of a 200-m LAR prototype is pursued by the National Research Council of Canada. Figure 1 is an artist's concept of a complete 200-m diameter LAR installation, which consists of two central components. The first is a 200-m diameter parabolic reflector with a focal length of 500 m, composed of actuated panels supported by the ground. The second component is the receiver package which is supported by a tension structure consisting of multiple long tethers and a helium-filled aerostat as shown schematically in Fig. 2. With funding from the Canada Foundation for Innovation, a one-third scale prototype of the multi-tethered aerostat subsystem has been designed and implemented in Penticton [4]. It should be noted that, even at one-third scale, this system is very large, with a footprint of roughly 1 km^2.

The challenging problem in this system is accurately positioning the feed (receiver) in the presence of disturbances, such as wind turbulence. As depicted in

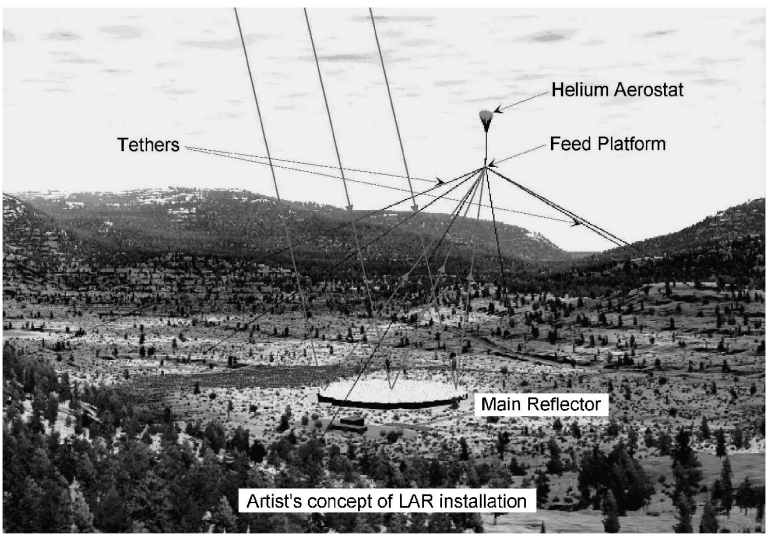

Figure 1. An artist's concept of a complete 200-m diameter LAR installation.

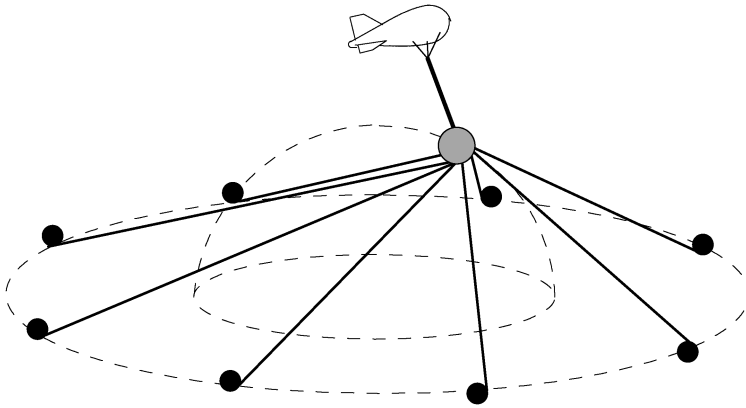

Figure 2. The schematics of the LCM with eight cables and aerostat.

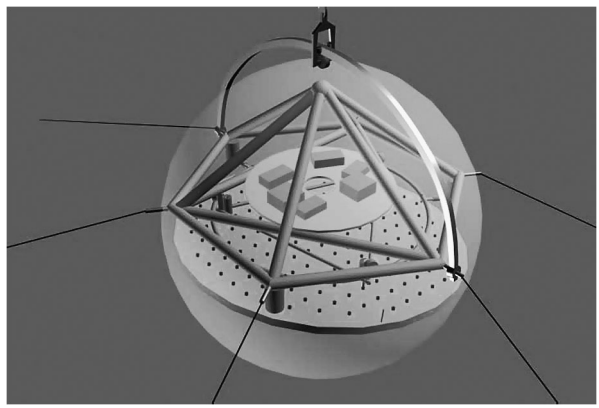

Figure 3. An artist concept of the CPM.

Figs 3 and 4, for the positioning structure of the receiver a macro–micro manipulator design is proposed, in which at both macro and micro levels two redundantly actuated cable-driven parallel manipulators are used. As illustrated in Fig. 2, at the macro level the receiver is moved to various locations on a circular hemisphere and its positioning is controlled by changing the lengths of eight tethers with ground winches. The cable-driven macro manipulator used in this design, which is called the Large Cable Mechanism (LCM), is in fact a 6-d.o.f. cable-driven redundantly actuated manipulator. Once the receiver is in place, the micro-level position control of the system responds to disturbances such as wind gusts in order to limit the movement of the receiver to centimeter accuracy. As is illustrated in Fig. 3 at the micro level a Confluence Point Mechanism (CPM) is designed to perform the final small-scale corrections at high frequencies. Figure 3 is an artist illustration of the CPM and the final design of the CPM is schematically illustrated in Fig. 4. The CPM requires 6 d.o.f. and, as schematically shown in Fig. 4, it is also designed as a redundantly actuated cable-driven parallel manipulator. As shown in Fig. 4, the

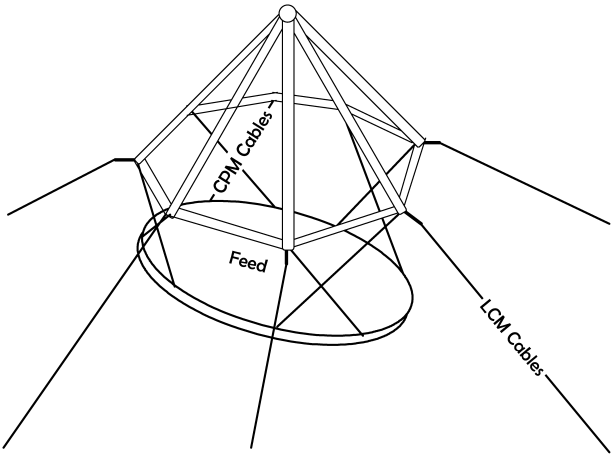

Figure 4. The schematics of the CPM with eight cables.

CPM base structure is attached to the LCM moving platform. This design is intended to keep the moving platform of the CPM and, hence, the feed, as close to stationary as possible and pointed toward the center of the reflector. The desired positioning accuracy of the feed in the real LAR application is in order of 1 cm, which is quite challenging to obtain, considering the LCM dimensions of about 500 m, and experimentally measured wind gust disturbances of about 10^5 N [5].

Since in the design of the LCM/CPM a macro–micro structure is proposed in which at each level a redundantly actuated parallel manipulator is used for extreme positioning accuracy, this paper is intended to study the kinematic analysis of such macro–micro structures in detail. Although the analysis of the above system is naturally adopted from the design of the LCM/CPM structure, it touches two leading topics in parallel robotics research, i.e., tendon-driven redundant parallel manipulators and the macro/micro structure in parallel structures, which have their own merits and potential applications beyond the LAR. In the LCM/CPM structure, two parallel manipulators with 6 d.o.f. are used at the macro and micro levels. In contrast to the open-chain macro–micro manipulator, the kinematic analysis of parallel manipulators with such structures exhibits an inherent complexity, due to their closed-loop and kinematic constraints. Therefore, in order to keep the analysis complexity at a managable level, while preserving all the important analysis elements, a simplified version of the LAR structure is considered in this paper as the base of the analysis. This structure is composed of two planar 4RPR parallel mechanisms, both actuated by cables. This mechanism is described in detail in the next section. In this simplified structure, although a planar version of the mechanisms is considered, two important features of the original design, i.e., the actuator redundancy for each subsystem and the macro–micro structure of the original design, are employed.

In the literature on kinematic analysis of parallel manipulator, mostly 6-d.o.f. parallel mechanisms based on the Stewart–Gough platform are analyzed [6, 7]. However, parallel manipulators with 3 d.o.f. have also been implemented for applications where 6 d.o.f. are not required. For a cable-driven manipulator though, at least one degree of redundancy is necessary to make sure that in all configurations all the cables are in tension [8, 9]. Complete kinematic modeling and Jacobian analysis of such mechanisms has not received much attention so far, and is still regarded as a challenging problem in parallel robotics research. It is known that unlike serial manipulators, inverse position kinematics for parallel robots is usually simple and straightforward. In most cases limb variables may be computed independently using the given pose of the moving platform and the solution in most cases is uniquely determined. However, the forward kinematics of parallel manipulators is generally very complicated and its solution usually involves systems of non-linear equations, which are highly coupled and in general have no closed form and unique solution. Different approaches are given in the literature to solve this problem either in general [10] or in special cases [11, 12]. Analysis of two such special 3-d.o.f. constrained mechanisms have been studied in Refs [13, 14]. In general, different solutions to the forward kinematics problem of parallel manipulators can be found using numerical [10] or analytical approaches [12]. In the Jacobian analysis of the parallel manipulator [15] is maybe the first to suggest the use of two Jacobian matrices in order to specify inverse and forward kinematics singularities. This analysis is performed for planar parallel manipulators in Ref. [16]. Screw theory has also been used to derive Jacobian matrices in parallel structures [17]. Among the various research areas performed in parallel manipulators, very few have analyzed parallel manipulators with a macro–micro structure [18, 19]. It is interesting to note that in Ref. [19] the macro–micro structure is also proposed for a Chinese concept of the LAR design.

Due to the potential attraction of the macro–micro structure in the LAR application, a thorough analysis of the kinematics and dynamics of the described macro–micro parallel manipulator has been developed, and some closed-loop control topologies are proposed and simulated for this system. In this paper the kinematic and Jacobian analysis of this system is reported in detail. Although such analysis for a macro–micro structure is rarely reported in the literature, and it has its own merits and importance, this analysis is extremely important to optimally design the geometry and characteristics of the LCM/CPM structure. The optimal location of the base and moving platform attachment points in both the LCM and CPM structures, singularity avoidance of the system in the nominal and extreme maneuvers, and geometries that result in high-dexterity measures in the design are among the few characteristics that can be further investigated from the general results reported in this paper. Furthermore, the availability of the extra degrees of freedom in a macro–micro structure can result in higher dexterity provided that this redundancy is properly utilized. In this paper, this redundancy is used to generate an optimal trajectory for the macro–micro manipulator. Furthermore, redundancy

resolution techniques can be applied to optimally utilize these extra degrees of freedom in control strategies. Finally, inverse kinematic formulation and macro–micro Jacobian matrices derived in this paper are extensively used in the dynamic modeling and control topologies reported separately elsewhere (Ref. [20] and data not shown).

2. Mechanism Description

The architecture of the planar macro–micro manipulator considered for our studies is denoted by a 2×4RPR parallel manipulator and is shown in Fig. 5. This manipulator consists of two similar 4RPR parallel structures at the macro and micro level. At both levels the moving platform is supported by four limbs of identical kinematic structure. The kinematic structure used to model the cable-driven limb is RPR, in which each limb connects the base to the moving platform by a revolute joint (base attachment points A_is or a_is) followed by a prismatic joint (limb elongation) and another revolute joint (moving platform attachment points B_is or b_is). In order to avoid singularities at the central position of the manipulator at each level, the cable-driven limbs are considered to be crossed as shown in the Fig. 5. A complete singularity analysis indicating the singularity-free design in the whole workspace is presented later in Section 4. At the micro level a similar 4RPR structure is used; however, the base points of the macro manipulators are located on the moving platform of the macro manipulator.

For the purpose of analysis and as illustrated in Fig. 6 for macro manipulators, a fixed frame O: xy is attached to the fixed base at the point O, the center of the base point circle which passes through A_is, and another moving coordinate

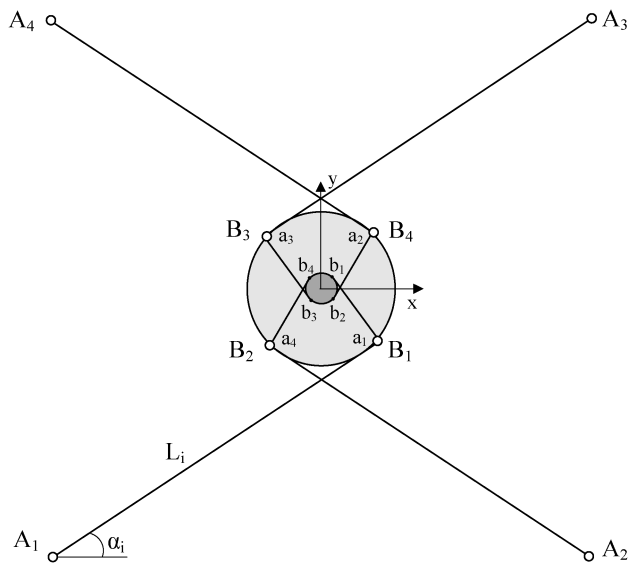

Figure 5. The schematics of 2×4RPR kinematic structure employed for the analysis of the LCM/CPM.

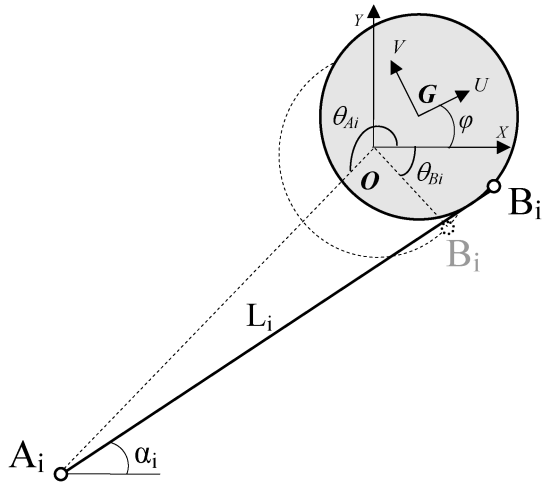

Figure 6. Geometry and variables used in the kinematic analysis of the macro–micro manipulator.

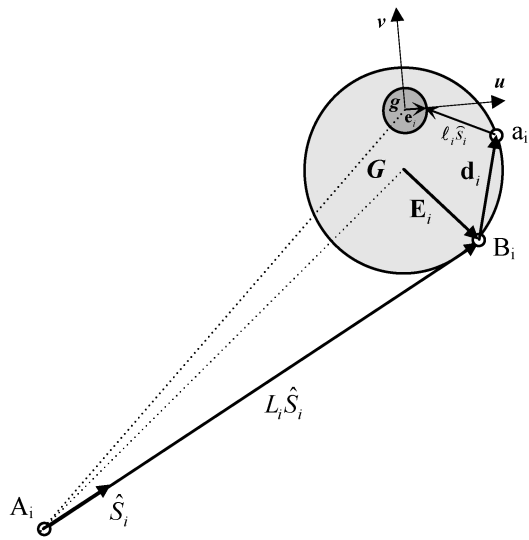

Figure 7. Vector definitions for Jacobian analysis of the macro–micro manipulator.

frame G: UV is attached to the macro manipulator moving platform at point G. Furthermore, assume that the point A_i lies at the radial distance of R_A from point O and the point B_i lies at the radial distance of R_B from point G in the xy plane, when the manipulator is at central location. Similarly for the micro manipulator as illustrated in Fig. 7, consider the micro moving coordinate frame g: uv which is attached to the micro manipulator moving platform at point g, the center of the micro moving platform. Furthermore, assume that the point a_i lies at the radial distance of R_a from point G and the point b_i lies at the radial distance of R_b from point g in the uv plane.

As illustrated in Fig. 6, in order to specify the geometry of the macro manipulator, define $\theta_{A_i}, \theta_{B_i}$ as the absolute angle of the points A_i and B_i at the central configuration of the macro manipulator with respect to the fixed frame O. Similarly, define $\theta_{a_i}, \theta_{b_i}$ as the absolute angle of the points a_i and b_i at the central configuration of the manipulator, with respect to the fixed frame O. The geometry of the fixed and moving platform attachment points, A_i, B_i, a_i and b_is, are considered to be arbitrary in the analysis and they are not necessarily coincident. However, the parameter used in the simulations of the system is adopted from the LCM/CPM design and is symmetrical as shown in Fig. 5 and given in Table 1. Note that throughout the analysis capital letters are used to describe the macro manipulator variables, while small letters are reserved for that of the micro manipulator. Furthermore, as illustrated in Fig. 6, in this representation L_i denotes the macro limb lengths, α_i denotes the macro limb angles, ℓ_i denotes the micro limb lengths and β_i denotes the micro limb angles. The position of the center of the moving platform G at the macro level is denoted by $G = [x_G, y_G]$ and the final position of the micro manipulator g is denoted by $g = [x_g, y_g]$. The orientation of the macro manipulator moving platform is denoted by ϕ and the orientation of the micro manipulator with respect to the fixed coordinate frame A, is denoted by ψ.

In this analysis it is assumed that the gravity vector is in the z direction, perpendicular to the plane of manipulation; hence, cable deflections due to gravity do not contribute in the planar motion. Furthermore, it is assumed that the cables can be kinematically modeled as straight lines. Experimental observations show that this assumption is valid for LAR applications [5, 21], due to the inherent pre-tension of the cables. However, in general, the sagging deflections of the tethers can be further included in the analysis as a modeling uncertainty. The kinematic analysis would

Table 1.
Geometric parameters of the macro–micro manipulator used in the simulations

Description	Symbols	Quantity
Location circle radius of the macro fixed points A_is	R_A	900 m
Location circle radius of the macro moving platform points B_is	R_B	10 m
Location circle radius of the micro fixed points a_is	R_a	10 m
Location circle radius of the micro moving platform points b_is	R_b	2 m
Angles of macro fixed points A_is	θ_{A_i}	$[-135°, -45°, 45°, 135°]$
Angles of macro moving platform points B_is	θ_{B_i}	$[-45°, -135°, 135°, 45°]$
Angles of micro fixed points a_is	θ_{a_i}	$[-45°, 45°, 135°, -135°]$
Angles of micro moving platform points b_is	θ_{b_i}	$[45°, -45°, -135°, 135°]$

be the same as in this case, but in the controller design robust schemes can be used to compensate for the sagging effect in such cases [22].

3. Kinematic Analysis

In this section, the kinematics of the system is studied in detail. In this analysis first the inverse and forward kinematic analysis of the macro manipulator is elaborated in detail, and then the kinematics of the macro–micro assembly is analyzed. In order to verify the formulations, in Section 3.4 the simulation results for computation of the inverse kinematics and forward kinematics of the macro–micro manipulator are presented, and the accuracy of the numerical solution to the forward kinematics is verified in detail.

3.1. Inverse Kinematics of the Macro Manipulator

For inverse kinematic analysis of the macro manipulator, it is assumed that the position and orientation of the moving platform $\mathbf{X} = [x_G, y_G, \phi]^{\mathrm{T}}$ is given and the problem is to find the joint variable of the macro manipulator, $\mathbf{L} = [L_1, L_2, L_3, L_4]^{\mathrm{T}}$. Let us define the instantaneous orientation angle of B_is as:

$$\phi_i = \phi + \theta_{B_i}. \tag{1}$$

For each limb, $i = 1, 2, \ldots, 4$, the position of the base points, A_i, is given by:

$$A_i = [R_A \cos(\theta_{A_i}), R_A \sin(\theta_{A_i})]^{\mathrm{T}}. \tag{2}$$

From the geometry of the macro manipulator as illustrated in Fig. 6, the loop-closure equation for each limb, $i = 1, 2, \ldots, 4$, can be written as:

$$\overrightarrow{A_iG} = \overrightarrow{A_iB_i} + \overrightarrow{B_iG}. \tag{3}$$

Rewriting the vector loop-closure component-wise:

$$x_G - x_{A_i} = L_i \cos(\alpha_i) - R_B \cos(\phi_i) \tag{4}$$

$$y_G - y_{A_i} = L_i \sin(\alpha_i) - R_B \sin(\phi_i), \tag{5}$$

in which α_i are the absolute limb angles. To solve the inverse kinematic problem it is required to eliminate α_is from the above equation and solve for L_is. This can be accomplished by reordering and adding the square of both sides of (4) and (5). Hence, the limb lengths are uniquely determined by:

$$L_i = \left[\left(x_G - x_{A_i} + R_B \cos(\phi_i)\right)^2 + \left(y_G - y_{A_i} + R_B \sin(\phi_i)\right)^2\right]^{1/2}. \tag{6}$$

Furthermore, the limb angles α_is can be determined by:

$$\alpha_i = \tan^{-1}\left(\left(y_G - y_{A_i} + R_B \sin(\phi_i)\right)/\left(x_G - x_{A_i} + R_B \cos(\phi_i)\right)\right). \tag{7}$$

Hence, corresponding to each given macro manipulator location vector $\mathbf{X} = [x_G, y_G, \phi]^{\mathrm{T}}$, there is a unique solution for the limb length L_is and limb angles α_is. Due to the nature of cable-driven actuators, the mechanism experiences no singularities at the boundaries of the workspace, since the actuator lengths can be extended without any limits.

3.2. Forward Kinematics of the Macro Manipulator

For the forward kinematic problem the joint variable L_is are given, and the position and orientation of the moving platform $\mathbf{X} = [x_G, y_G, \phi]^{\mathrm{T}}$ of the macro manipulator are to be found. This can be accomplished by eliminating x_G and y_G from (4) and (5) as follows. Let us define two intermediate variables $x_i = -x_{A_i} + R_B \cos(\phi_i)$ and $y_i = -y_{A_i} + R_B \sin(\phi_i)$ in order to simplify the calculations and consider the square of (6):

$$L_i^2 = (x_G + x_i)^2 + (y_G + y_i)^2. \tag{8}$$

We first try to solve for x_G and y_G. This can be accomplished by reordering (8) into:

$$x_G^2 + y_G^2 + r_i x_G + s_i y_G + u_i = 0, \tag{9}$$

in which for $i = 1, 2, \ldots, 4$:

$$\begin{cases} r_i = 2x_i \\ s_i = 2y_i \\ u_i = x_i^2 + y_i^2 - L_i^2. \end{cases} \tag{10}$$

Equation (9) provides four quadratic relations for x_G and y_G for $i = 1, 2, \ldots, 4$. Subtracting each two equations from each other results into a linear equation in terms of x_G and y_G:

$$\mathbf{A} \cdot \begin{bmatrix} x_G \\ y_G \end{bmatrix} = \mathbf{b}, \tag{11}$$

in which:

$$\mathbf{A} = \begin{bmatrix} r_1 - r_2 & s_1 - s_2 \\ r_2 - r_3 & s_2 - s_3 \\ r_3 - r_4 & s_3 - s_4 \\ r_4 - r_1 & s_4 - s_1 \end{bmatrix}, \qquad \mathbf{b} = \begin{bmatrix} u_2 - u_1 \\ u_3 - u_2 \\ u_4 - u_3 \\ u_1 - u_4 \end{bmatrix}. \tag{12}$$

The components of $\mathbf{A}$ and $\mathbf{b}$ are all functions of ϕ. Note that only the two equations above could be used to evaluate x_G and y_G in terms of ϕ, but all the possible four equations are used in here to have tractable solutions even in case of configuration singularities in the manipulator. Over-determined (11) can be solved using the pseudo-inverse:

$$\begin{bmatrix} x_G \\ y_G \end{bmatrix} = \mathbf{A}^{\dagger} \cdot \mathbf{b}, \tag{13}$$

in which $A^{\dagger}$ denotes the pseudo-inverse solution of A and for an over-determined set of equations this is calculated from:

$$A^{\dagger} = (A^{\mathrm{T}} A)^{-1} A^{\mathrm{T}}. \tag{14}$$

There exist tractable numerical methods such as Householder reflection or Choleski decomposition (pinv function of Matlab) to evaluate the pseudo-inverse. Note that

the components of **A** and **b** are all functions of ϕ, and for a given ϕ (13) gives the least-squares solution for x_G and y_G. In order to solve for ϕ this solution can be substituted in (9), and a function of the only unknown variable ϕ is obtained:

$$f_i(\phi) = x_G^2 + y_G^2 + r_i x_G + s_i y_G + u_i \tag{15}$$

$$f(\phi) = \sum_{i=1}^{4} f_i(\phi). \tag{16}$$

Numerical methods using iterative search routines (fzero function of Matlab) can be used to find the final solution of $f(\phi) = 0$. Notice that any function $f_i(\phi) = 0$ could be used to find ϕ which solves the forward kinematics; however, the summation of all four possible equations is used in here to have a tractable solution even in the case of a singularity in the manipulator configuration. The flowchart given in Fig. 8 reveals the details of the iterative method used to find the forward kinematic solution. A multiple solution may exist for the equation $f(\phi) = 0$ and in order to avoid jumps in the forward kinematic solutions, in the numerical routine the solution at the previous iteration is used for the search of the next solution. Simulation results detailed in Section 3.4 illustrate the effectiveness and accuracy of the nu-

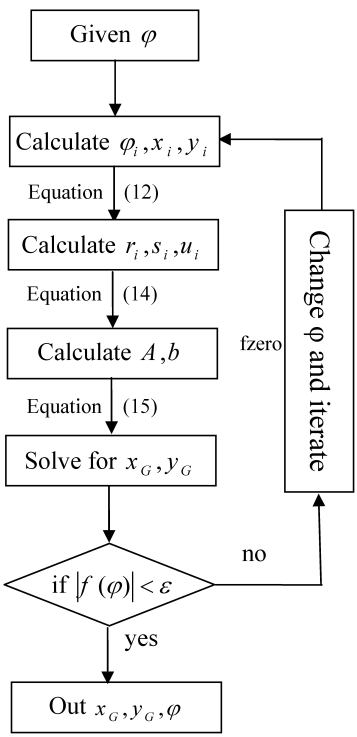

Figure 8. Flowchart of the iterative routine used to solve the forward kinematics of the macro manipulator.

merical routines used to solve forward kinematics. If the limb angles α_is need to be found (7) can be used directly, by substituting x_G, y_G and ϕ.

3.3. Macro–Micro Kinematics

For inverse kinematic analysis of the macro–micro manipulator, it is assumed that the location vector of the macro moving platform $\mathbf{X} = [x_G, y_G, \phi]^{\mathrm{T}}$ and that of the micro moving platform $\mathbf{x} = [x_g, y_g, \psi]^{\mathrm{T}}$ is given. The problem is then to find the joint variable of the macro manipulator $\mathbf{L} = [L_1, L_2, L_3, L_4]^{\mathrm{T}}$ and micro manipulator $\boldsymbol{\ell} = [\ell_1, \ell_2, \ell_3, \ell_4]^{\mathrm{T}}$, respectively. As explained previously, capital letters are reserved for the macro manipulator variables, while small letters are used to denote the micro manipulator variables.

Since the structures of the macro and micro manipulators are the same, the inverse kinematic solution of the macro–micro system is similar to that of the macro manipulator and can be found in the following sequence. Starting with the macro manipulator inverse kinematic solution, for a given $\mathbf{X} = [x_G, y_G, \phi]^{\mathrm{T}}$, the macro joint variables L_is, and α_is are determined from (6) and (7), respectively. Then the macro moving platform points coordinate B_is and a_is are determined from the following geometrical relation:

$$B_i = [x_G + R_B \cos(\theta_{B_i} + \phi),\, y_G + R_B \sin(\theta_{B_i} + \phi)]^{\mathrm{T}} \tag{17}$$

$$a_i = [x_G + R_a \cos(\theta_{a_i} + \phi),\, y_G + R_a \sin(\theta_{a_i} + \phi)]^{\mathrm{T}}. \tag{18}$$

Finally, assuming that the micro manipulator position and orientation $[x_g, y_g, \psi]^{\mathrm{T}}$ is given, the micro manipulator joint variables can be determined by the following equations, similar to that to the macro manipulator (6) and (7):

$$\ell_i = \left[\left(x_g - x_{a_i} + R_b \cos(\psi_i)\right)^2 + \left(y_g - y_{a_i} + R_b \sin(\psi_i)\right)^2\right]^{1/2}, \tag{19}$$

in which:

$$\psi_i = \psi + \theta_{b_i}. \tag{20}$$

Furthermore the micro manipulator limb angles β_is can be determined from:

$$\beta_i = \tan^{-1}\left(\left(y_g - y_{a_i} + R_b \sin(\psi_i)\right)/\left(x_g - x_{a_i} + R_b \cos(\psi_i)\right)\right). \tag{21}$$

The forward kinematic solution of the macro–micro manipulator can be solved by parallel computation, too. For the forward kinematic problem the joint variable L_is and ℓ_is are given, and the position and orientation of the macro moving platform $\mathbf{X} = [x_G, y_G, \phi]^{\mathrm{T}}$ and that of micro manipulator $\mathbf{x} = [x_g, y_g, \psi]^{\mathrm{T}}$ are to be found. Similar to (4) and (5) for the micro manipulator, the vector loop closure results:

$$\ell_i \cos(\beta_i) = x_g - x_{a_i} + R_b \cos(\psi_i) \tag{22}$$

$$\ell_i \sin(\beta_i) = y_g - y_{a_i} + R_b \sin(\psi_i). \tag{23}$$

Hence, a similar numerical solution for the macro manipulator can be determined with the identical equation used for the macro manipulator, i.e., (11) and (16), replacing the following variables:

$$\begin{cases} L_i, \alpha_i \longrightarrow \ell_i, \beta_i \\ \phi, \phi_i \longrightarrow \psi, \psi_i \\ x_G, y_G \longrightarrow x_g, y_g \\ x_A, y_A \longrightarrow x_a, y_a \\ x_B, y_B \longrightarrow x_b, y_b \\ R_A, R_B \longrightarrow R_a, R_b. \end{cases} \tag{24}$$

The sequence of the macro–micro forward kinematic solution is to first solve the macro manipulator forward kinematic. This can be accomplished as illustrated in the flowchart of Fig. 8. Similarly, ψ is numerically calculated solving (16), by substituting variables in (24), and then solving for x_g and y_g using (13) whose variables are substituted by (24). It is noticeable that due to the similar structures of the macro and micro manipulators, a complete kinematic solution of the system can be calculated in parallel for macro and micro manipulators. Moreover, identical subroutines can be used to solve the individual kinematic problems more efficiently.

3.4. Kinematics Verification

The inverse and forward kinematic analysis of the macro–micro manipulator is given in Section 3 in detail. In order to verify the accuracy and integrity of the numerical solutions, for a given trajectory for the micro manipulator, x_{d} the desired trajectory for the macro manipulator is derived using the optimal trajectory planning with minimal micro motion criteria, which will be explained in Section 5.1. By this means the desired trajectories X_{d} and x_{d} are found to be identical. The trajectories being used in here are illustrated in Fig. 9. The inverse kinematic solution of the macro–micro manipulator is found by (6) and (19), and the macro manipulator limb lengths are uniquely derived and illustrated in Fig. 10. It is shown that due to minimal micro motion criteria in trajectory planning, there is no relative motion observed in the micro manipulator and, hence, the micro limb lengths are constant at all times. Macro limb length changes, however, according to the desired trajectory variation. In order to verify the accuracy and integrity of the numerical solutions, the forward kinematic solutions for the macro and micro manipulators are found by the sequence depicted in the flowchart in Fig. 8. It is observed that the calculated numerical solutions from the forward kinematic problem are completely identical to the desired trajectories given to an accuracy of 10^{-13} for the macro manipulator and 10^{-12} for the micro manipulator. It should be noted that the forward kinematic solutions are not unique and to avoid converging to the other solutions at each step of time the last step of the forward kinematic solution is used as the initial guess for the next step iteration. By this means the numerical solution converges to the right solution in all the examined points. Moreover, it is noticeable that due to the similar structures of the macro and micro manipulators, complete kinematic solution of the system can be calculated in parallel for the macro and micro manipulators,

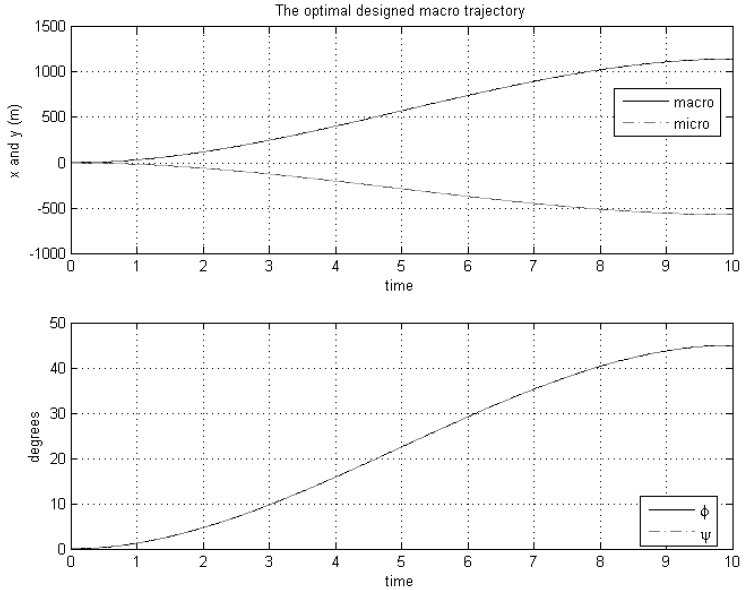

Figure 9. Optimal trajectory solution for micro minimal motion criteria: macro and micro absolute position and orientation.

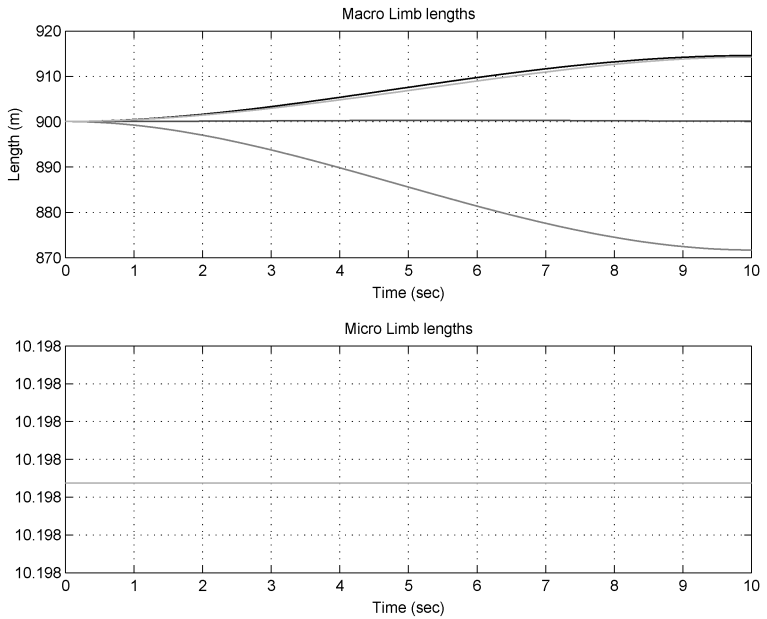

Figure 10. Inverse kinematic solution for the given trajectory.

and identical subroutines are used to solve the individual kinematic problems very efficiently.

4. Jacobian Analysis

Jacobian analysis plays a vital role in the study of robotic manipulators. The Jacobian matrix not only reveals the relation between the joint variable velocities $\dot{\mathbf{L}}$ and the moving platform velocities $\dot{\mathbf{X}}$, it constructs the transformation needed to find the actuator forces $\boldsymbol{\tau}$ from the forces acting on the moving platform $\mathbf{F}$. In this section the Jacobian analysis for the macro manipulator is performed first in Section 4.1. Then, the Jacobian matrix of the macro–micro manipulator is derived and analyzed in Section 4.2. The system Jacobian is then used in the singularity analysis and the optimal trajectory planning of the macro–micro manipulator in Sections 4.3 and 5, respectively.

4.1. Macro Jacobian

Contrary to serial manipulators, the Jacobian matrix of a parallel manipulator is defined as the transformation matrix that converts the moving platform velocities to the joint variable velocities, i.e.:

$$\dot{\mathbf{L}} = \mathbf{J}_M \cdot \dot{\mathbf{X}}, \tag{25}$$

in which for the macro manipulator $\dot{\mathbf{L}} = [\dot{L}_1, \dot{L}_2, \dot{L}_3, \dot{L}_4]$ is the 4×1 limb velocity vector and $\dot{\mathbf{X}} = [\dot{x}_G, \dot{y}_G, \dot{\phi}]$ is the 3×1 moving platform velocity vector. Therefore, the macro Jacobian matrix $\mathbf{J}_M$ is a non-square 4×3 matrix. In order to obtain the Jacobian matrix, let us differentiate the vector loop (3) with respect to time, considering the vector definitions $\hat{\mathbf{S}}_i$ and $\mathbf{E}_i$ illustrated in Fig. 7. Hence, for $i = 1, 2, \ldots, 4$:

$$\mathbf{v}_G + \dot{\phi}(\hat{\mathbf{K}} \times \mathbf{E}_i) = \dot{L}_i \hat{\mathbf{S}}_i + \dot{\alpha}_i L_i (\hat{\mathbf{K}} \times \hat{\mathbf{S}}_i), \tag{26}$$

in which $\mathbf{v}_G = [\dot{x}_G, \dot{y}_G]^{\mathrm{T}}$ is the velocity of the moving platform at point G and $\hat{K}$ is the unit vector in the Z direction of the fixed coordinate frame O. In order to eliminate $\dot{\alpha}_i$, dot multiply both sides of (26) with $\hat{S}_i$:

$$\hat{S}_i \cdot \mathbf{v}_G + \hat{\mathbf{K}} \cdot (\mathbf{E}_i \times \hat{\mathbf{S}}_i)\dot{\phi} = \dot{L}_i. \tag{27}$$

Rewriting (27) in a matrix form:

$$\dot{L}_i = \left[\begin{array}{c|c|c} S_{ix} & S_{iy} & E_{ix}S_{iy} - E_{iy}S_{ix} \end{array} \right] \cdot \begin{bmatrix} v_{Gx} \\ v_{Gy} \\ \dot{\phi} \end{bmatrix}. \tag{28}$$

Using (28) for $i = 1, 2, \ldots, 4$ the macro Jacobian matrix J_M is derived:

$$\mathbf{J}_M = \left[\begin{array}{c|c|c} S_{1x} & S_{1y} & E_{1x}S_{1y} - E_{1y}S_{1x} \\ S_{2x} & S_{2y} & E_{2x}S_{2y} - E_{2y}S_{2x} \\ S_{3x} & S_{3y} & E_{3x}S_{3y} - E_{3y}S_{3x} \\ S_{4x} & S_{4y} & E_{4x}S_{4y} - E_{4y}S_{4x} \end{array} \right] \tag{29}$$

note that the macro Jacobian matrix $\mathbf{J}_M$ is a non-square 4×3 matrix, since the manipulator is a redundant manipulator.

4.2. Macro–Micro Jacobian

As is illustrated in Fig. 7, denote $\hat{\mathbf{s}}_i$ as the unit vector along the micro manipulator limb i, $\mathbf{e}_i$ the vector from point g to b_i and $\mathbf{d}_i$ as the vector from point B_i to the point a_i. The vector loop closure for the micro manipulator can be written as:

$$\overrightarrow{A_i g} + \overrightarrow{g b_i} = \overrightarrow{A_i B_i} + \overrightarrow{B_i a_i} + \overrightarrow{a_i b_i}. \tag{30}$$

Substitute $\overrightarrow{A_i B_i}$ from (3):

$$\overrightarrow{A_i g} + \overrightarrow{g b_i} = \overrightarrow{A_i G} + \overrightarrow{G B_i} + \overrightarrow{B_i a_i} + \overrightarrow{a_i b_i}. \tag{31}$$

Differentiate both sides with respect to time:

$$\mathbf{v}_g + \dot{\psi}(\hat{\mathbf{K}} \times \mathbf{e}_i) = \mathbf{v}_G + \dot{\phi}(\hat{\mathbf{K}} \times \mathbf{E}_i) + \dot{\phi}(\hat{\mathbf{K}} \times \mathbf{d}_i) + \dot{\ell}_i \hat{\mathbf{s}}_i + \dot{\beta}_i \ell_i (\hat{\mathbf{K}} \times \hat{\mathbf{s}}_i). \tag{32}$$

Dot multiply to $\hat{\mathbf{s}}_i$ to eliminate $\dot{\beta}$:

$$\hat{\mathbf{s}}_i \cdot \mathbf{v}_g + \dot{\psi} \hat{K} \cdot (\mathbf{e}_i \times \hat{\mathbf{s}}_i) = \hat{\mathbf{s}}_i \cdot \mathbf{v}_G + \dot{\phi} \hat{K} \cdot \big((\mathbf{E}_i + \mathbf{d}_i) \times \hat{\mathbf{s}}_i\big) + \dot{\ell}_i. \tag{33}$$

Rewriting (33) into a matrix form:

$$\begin{aligned} &\left[\, s_{ix} \;\middle|\; s_{iy} \;\middle|\; e_{ix}s_{iy} - e_{iy}s_{ix} \,\right] \cdot \begin{bmatrix} v_{gx} \\ v_{gy} \\ \dot{\psi} \end{bmatrix} \\ &\quad = \left[\, s_{ix} \;\middle|\; s_{iy} \;\middle|\; (E_{ix} + d_{ix})s_{iy} - (E_{iy} + d_{iy})s_{ix} \,\right] \cdot \begin{bmatrix} v_{Gx} \\ v_{Gy} \\ \dot{\phi} \end{bmatrix} + \dot{\ell}_i. \end{aligned} \tag{34}$$

Using (34) for $i = 1, 2, \ldots, 4$, define two different Jacobian matrices, $\mathbf{J}_m$ the micro manipulator Jacobian and $\mathbf{J}_{M_m}$ the macro–micro coupled Jacobian, as:

$$\mathbf{J}_m = \left[\begin{array}{c|c|c} s_{1x} & s_{1y} & e_{1x}s_{1y} - e_{1y}s_{1x} \\ s_{2x} & s_{2y} & e_{2x}s_{2y} - e_{2y}s_{2x} \\ s_{3x} & s_{3y} & e_{3x}s_{3y} - e_{3y}s_{3x} \\ s_{4x} & s_{4y} & e_{4x}s_{4y} - e_{4y}s_{4x} \end{array}\right] \tag{35}$$

$$\mathbf{J}_{M_m} = \left[\begin{array}{c|c|c} s_{1x} & s_{1y} & (E_{1x} + d_{1x})s_{1y} - (E_{1y} + d_{1y})s_{1x} \\ s_{2x} & s_{2y} & (E_{2x} + d_{2x})s_{2y} - (E_{2y} + d_{2y})s_{2x} \\ s_{3x} & s_{3y} & (E_{3x} + d_{3x})s_{3y} - (E_{3y} + d_{3y})s_{3x} \\ s_{4x} & s_{4y} & (E_{4x} + d_{4x})s_{4y} - (E_{4y} + d_{4y})s_{4x} \end{array}\right]. \tag{36}$$

Hence:

$$\mathbf{J}_m \cdot \dot{\mathbf{x}} = \mathbf{J}_{M_m} \cdot \dot{\mathbf{X}} + \dot{\boldsymbol{\ell}}. \tag{37}$$

Equation (37) constitutes the relation between the micro manipulator joint velocity vector $\dot{\boldsymbol{\ell}}$ to the macro and micro Cartesian space velocities $\dot{\mathbf{X}}$ and $\dot{\mathbf{x}}$. Moreover, the total macro–micro manipulator Jacobian matrix $\mathbf{J}_t$ can be defined as the projection matrix of total macro–micro joint velocities $\dot{\mathcal{L}} = [\dot{\mathbf{L}}^T, \dot{\boldsymbol{\ell}}^T]^T$ to the vector of the macro and micro moving platform velocities $\dot{\mathcal{X}} = [\dot{\mathbf{X}}^T, \dot{\mathbf{x}}^T]^T$ as:

$$\dot{\mathcal{L}} = \mathbf{J}_t \cdot \dot{\mathcal{X}}. \tag{38}$$

The 8×6 Jacobian matrix $\mathbf{J}_{\mathrm{t}}$ can be derived by grouping $\dot{\mathcal{L}}$ and $\dot{\mathcal{X}}$ from (25) and (37):

$$\mathbf{J}_{\mathrm{t}} = \begin{bmatrix} \mathbf{J}_M & \mathbf{0} \\ -\mathbf{J}_{M_m} & \mathbf{J}_m \end{bmatrix}. \tag{39}$$

As seen from this equation the total Jacobian matrix of the macro–micro manipulator is a block triangular matrix, which contains the macro and micro individual Jacobian matrices $\mathbf{J}_M$ and $\mathbf{J}_m$ as the diagonal blocks and the coupling Jacobian matrix $\mathbf{J}_{M_m}$ as the off-diagonal block.

4.3. Singularity Analysis

This section is devoted to the singularity analysis of the macro–micro parallel manipulator. The Jacobian analysis of the parallel manipulator is generally much more comprehensive than that of a serial manipulator. An important limitation of the parallel manipulator is that a singular configuration may exist within the workspace, where the manipulator can gain 1 d.o.f. or more and, therefore, loses its stiffness. Moreover, as suggested in Ref. [15], singularities of closed-loop mechanisms are separated by the analysis of two Jacobian matrices. In general the kinematic constraints imposed by the limbs can be written as:

$$\mathbf{f}(\boldsymbol{\mathcal{X}}, \boldsymbol{\mathcal{L}}) = \mathbf{0}, \tag{40}$$

in which $\mathbf{f}$ is an n-dimensional implicit function of joint space variable $\boldsymbol{\mathcal{L}}$ and Cartesian space variable $\boldsymbol{\mathcal{X}}$, and $\mathbf{0}$ is an n-dimensional zero vector. The two general Jacobian matrices for the parallel manipulator can be obtained by differentiation of (40) with respect to time:

$$\mathbf{J}_x \cdot \dot{\boldsymbol{\mathcal{X}}} = \mathbf{J}_{\mathcal{L}} \cdot \dot{\boldsymbol{\mathcal{L}}}, \tag{41}$$

where:

$$\mathbf{J}_x = \frac{\partial \mathbf{f}}{\partial \boldsymbol{\mathcal{X}}} \quad \text{and} \quad \mathbf{J}_{\mathcal{L}} = \frac{\partial \mathbf{f}}{\partial \boldsymbol{\mathcal{L}}}. \tag{42}$$

The manipulator is at a singular configuration when either $\mathbf{J}_x$ and $\mathbf{J}_{\mathcal{L}}$ or both are singular. Hence, three different type of singularities can be identified as is suggested in Ref. [15]. An inverse kinematic singularity occurs when the Jacobian matrix $\mathbf{J}_{\mathcal{L}}$ is rank deficient. When $\mathbf{J}_{\mathcal{L}}$ is singular and the null space of $\mathbf{J}_{\mathcal{L}}$ is non-empty, there exists some non-zero $\dot{\boldsymbol{\mathcal{L}}}$ that result in zero $\dot{\mathbf{x}}$. This means that infinitesimal motion of the moving platform along certain directions cannot be accomplished and the manipulator has lost 1 d.o.f. more. A direct kinematic singularity occurs when the Jacobian matrix $\mathbf{J}_x$ is rank deficient. When $\mathbf{J}_x$ is singular and the null space of $\mathbf{J}_x$ is non-empty, there exists some non-zero $\dot{\boldsymbol{\mathcal{L}}}$ that result in zero $\dot{\boldsymbol{\mathcal{X}}}$. That means that the moving platform can possess infinitesimal motion in some directions while all the actuators are locked. Hence, the manipulator gains 1 d.o.f. or more in this case. A combined singularity occurs when both $\mathbf{J}_{\mathcal{L}}$ and $\mathbf{J}_x$ become simultaneously rank deficient. Generally, this type of singularity can occur only for manipulators with special kinematic architecture.

To study the singularity analysis of the macro–micro manipulator at hand, first consider the macro manipulator. The Jacobian matrix of the macro 4RPR manipulator is given in (29). Considering the general Jacobian definition in (41) and comparing this to (25), it is clear that for the macro manipulator $\mathbf{J}_{\mathcal{L}} = \mathbf{I}$ and $\mathbf{J}_x = \mathbf{J}_M$. Hence, the macro manipulator has no inverse kinematic singularity, but may possess a direct kinematic singularity when $\mathbf{J}_M$ becomes rank deficient. Notice that since the macro manipulator is a redundant parallel manipulator and $\mathbf{J}_M$ is a 4×3 matrix, the system experiences a singular configuration when:

$$\det\left(\mathbf{J}_M^{\mathrm{T}} \cdot \mathbf{J}_M\right) = 0. \tag{43}$$

The singular configuration can be derived either by calculation of (43) at grid points in the entire manipulator workspace or examining the properties of the matrix $\mathbf{J}_M$ geometrically. By doing the latter, since $\mathbf{J}_M$ consists of three columns of $\hat{S}_x$, $\hat{S}_y$ and $\mathbf{E} \times \hat{\mathbf{S}}$, the matrix may become singular if either of the columns becomes zero or two columns become linearly dependent. Hence, from a geometrical representation of vectors $\mathbf{E}$ and $\hat{S}$, which is depicted in Fig. 7, $\mathbf{E} \times \hat{\mathbf{S}} = \mathbf{0}$ only if the two vectors becomes parallel. This can happen when, for example, at the central position when $x_G = y_G = 0$, the moving platform angle is $\phi = \pm 90^\circ$. When moving the platform away from the central position, geometric interpretation becomes non-trivial. Therefore, the complete singularity location for the macro manipulator is derived from calculation of (43), for a number of grid points in the workspace of the manipulator. This calculation has been done for 1089 grid points within $-50 \leqslant x_G \leqslant 50$, $-50 \leqslant y_G \leqslant 50$, and $-\pi \leqslant \phi \leqslant \pi$, and the singular configurations are given in the three-dimensional plot of Fig. 11. As seen in this Fig. 11, the geometrical interpretation of the singular configuration is confirmed and is extended to points in two planes where:

$$x_G = \pm y_G \quad \text{and} \quad \phi = \pm 90^\circ. \tag{44}$$

Note that in the design of the manipulators, the cable-crossed configuration is considered. The main reason for this choice is to avoid having a singular configuration at the central position and orientation $x_G = y_G = \phi = 0$. In this proposed design, the macro manipulator is singular free for its entire workspace, provided that the desired moving platform orientation angle is smaller than $\pm 90^\circ$.

For the macro–micro manipulator as given in (38) $\mathbf{J}_{\mathcal{L}} = \mathbf{I}$ and $\mathbf{J}_x = \mathbf{J}_{\mathrm{t}}$ as defined in (39). Hence, the macro–micro manipulator has no inverse kinematic singularity, but may possess a direct kinematic singularity when $\mathbf{J}_{\mathrm{t}}$ becomes rank deficient. Moreover, since $\mathbf{J}_{\mathrm{t}}$ is a block triangular matrix it becomes rank deficient when either of the diagonal blocks $\mathbf{J}_M$ and $\mathbf{J}_m$ or both are rank deficient. Hence, the rank deficiency of the coupled Jacobian matrix $\mathbf{J}_{M_m}$ does not contribute into the macro–micro singularities. Rank deficiency of the macro manipulator Jacobian matrix $\mathbf{J}_M$ is analyzed and its singular configurations are given in (44). Notice that

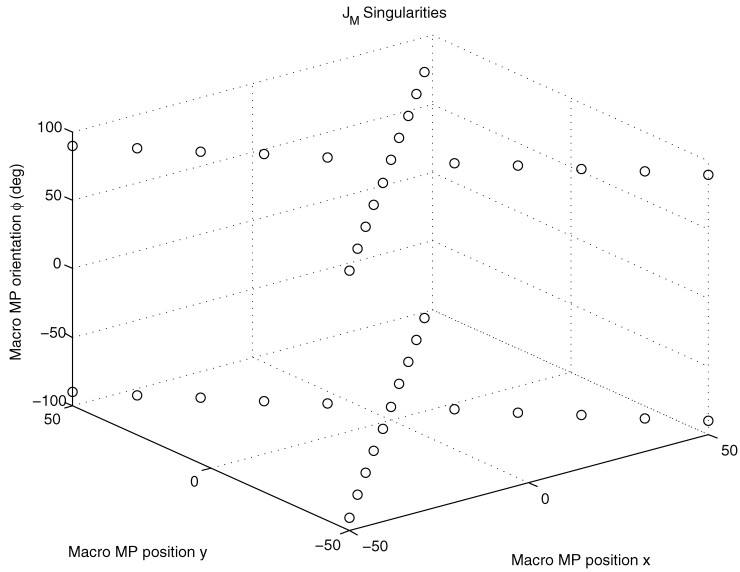

Figure 11. Singular configuration of the macro manipulator.

$\mathbf{J}_m$ has a similar structure to that of the macro manipulator Jacobian matrix $\mathbf{J}_M$ and its singularities occur when:

$$\det\left(\mathbf{J}_m^{\mathrm{T}} \cdot \mathbf{J}_m\right) = 0. \tag{45}$$

However, since $\mathbf{J}_m$s columns consist of the vectors, $\hat{s}_x$, $\hat{s}_y$ and $\mathbf{e} \times \hat{\mathbf{s}}$, and the direction of the vector $\hat{\mathbf{s}}$ depends on the relative position of the micro manipulator moving platform to that of the macro moving platform, the singular configurations are a function of the total Cartesian space vector $\boldsymbol{\mathcal{X}}$. A similar pattern of singularity configuration is observed for the micro manipulator, and is visualized in Figs 12 and 13. Figures 12 and 13 show the singularity configuration in the relative (x, y) plane and in the relative (x, y, ϕ) space. It is observed that a singular configuration occurs when:

$$\begin{aligned} &\left(x_G - x_g = \pm(y_G - y_g) \text{ or } x_G - x_g = 0 \text{ or } y_G - y_g = 0\right) \quad \text{and} \\ &\phi - \psi = \pm 90^\circ \text{ or } \pm 270^\circ. \end{aligned} \tag{46}$$

Since the singularity space for the macro manipulator is a six-dimensional space, the singularity configuration cannot be visualized in one figure and, therefore, Fig. 12 depict the singularity configurations only at the $(x_G - x_g, y_G - y_g)$ relative macro–micro motion plane. As seen in Fig. 12, a singularity occurs similar to that in the macro manipulator when the relative horizontal positions $x_G - x_g$ are equal to $\pm(y_g - y_g)$, or when the relative horizontal or vertical motions are equal to zero. Furthermore, the most important configuration variable where a singularity occurs depends on the relative orientation of the macro moving platform with respect to that of the macro manipulator. This is visualized in Fig. 13, where the

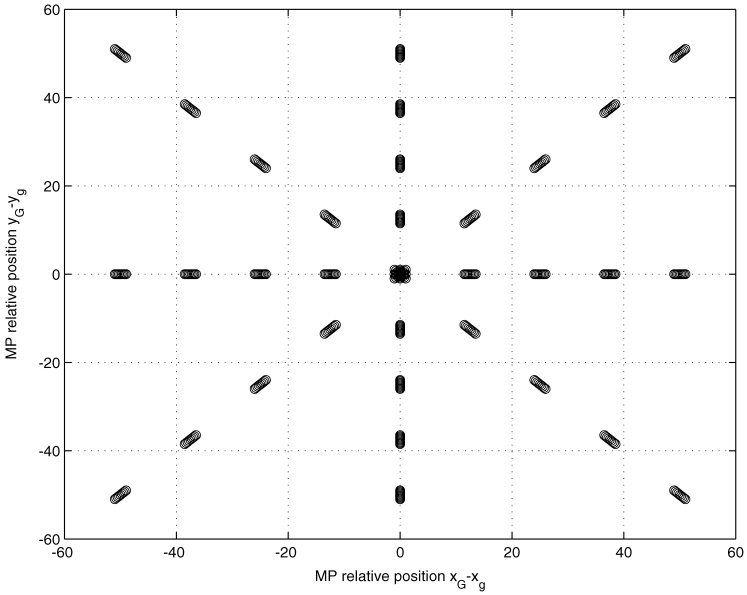

Figure 12. Singular configuration of the micro manipulator: $(x_G - x_g, y_G - y_g)$ plane.

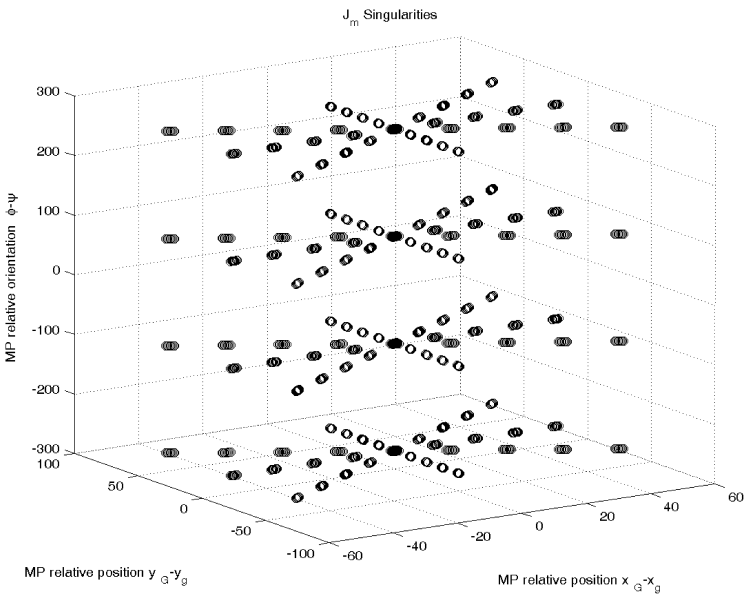

Figure 13. Singular configuration of the micro manipulator: $(x_G - x_g, y_G - y_g)$ *versus* relative orientation $(\phi - \psi)$.

singularity configurations are plotted for all $(x_G - x_g, y_G - y_g)$ positions as a function of relative orientation $\phi - \psi$. As seen in Fig. 13, a singularity happens when $\phi - \psi = \pm 90^\circ$ or $\pm 270^\circ$.

4.4. Sensitivity Analysis

As seen in the previous subsection, the singular points of the manipulator are limited to a few configurations where either $\phi = \pm 90°$ or in general where $\phi - \psi = \pm 90°$ or 270°. In this section the conditioning of the Jacobian matrices of the macro and micro–macro manipulator are analyzed in configurations close to the singular poses. The measure proposed to analyze the good conditioning of the manipulator Jacobian matrices is the inverse of the condition number of the Jacobian. In fact, for a non-square matrix, like the redundant manipulator Jacobian matrices, this measure quantifies the ratio of the smallest to the largest singular value of the matrix. If the system is close to a singular configuration the smallest singular value tends to 0, resulting in having a small value for the sensitivity measure. In contrast, values close to 1 for the sensitivity measure depict poses where the singular values are close to each other or the manipulator is in an isotropic configuration.

Figure 14 illustrates the sensitivity measure of the macro and micro manipulator Jacobian matrices for a typical trajectory. As illustrated in Fig. 14 (top), a typical trajectory is considered for the moving platform, in which the horizontal and vertical motion is about 100 m, while the orientation of the moving platform is about 180°. The initial orientation is very close to the −90° singular configuration and the final orientation is also close to the singular configuration of 90°. Figure 14 (bottom) gives a logarithmic scale plot of the sensitivity measure of the macro manipulator Jacobian $\mathbf{J}_M$, that for the micro manipulator $\mathbf{J}_m$ and, finally, that

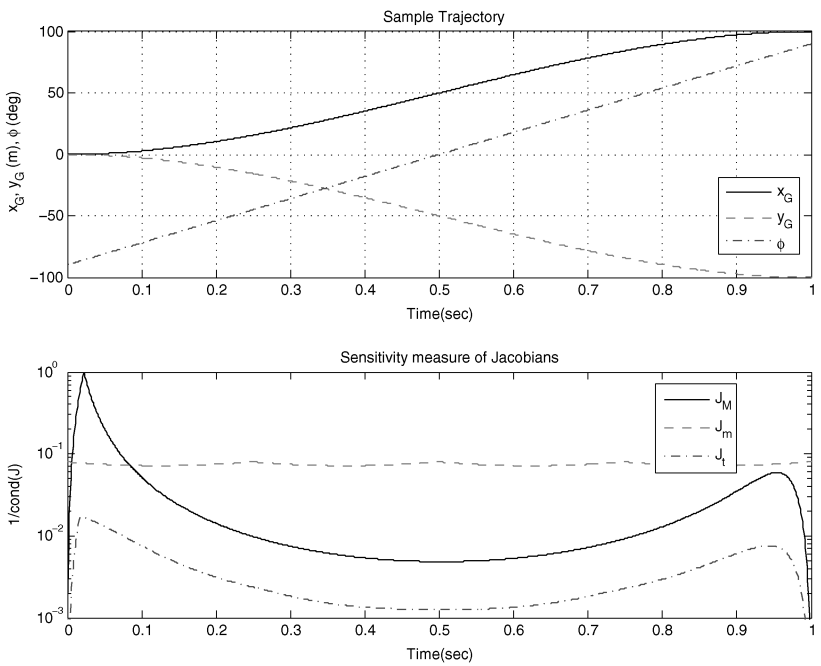

Figure 14. Sensitivity measure of the manipulator Jacobians with respect to a typical trajectory.

for the macro–micro total Jacobian $\mathbf{J}_t$ for this typical trajectory. As seen, the sensitivity measure of the macro manipulator Jacobian matrix $\mathbf{J}_M$ is close to zero at the initial and final configurations as expected for these singular configurations. However, the Jacobian matrix is well-conditioned as the trajectory moves away from the singular configuration. Moreover, the micro manipulator sensitivity measure is relatively higher close to singular configurations and, therefore, the micro manipulator Jacobian $\mathbf{J}_m$ is well-conditioned on the overall considered trajectory. The conditioning of the total Jacobian of the macro–micro manipulator $\mathbf{J}_t$ is a function of the individual macro and micro components, and is also illustrated. The variation of the sensitivity measure of the total Jacobian is similar to that to the macro manipulator, but the macro manipulator is quantitatively better conditioned. Since the sensitivity measures are given on a logarithmic scale, it is noticeable that for the configurations not very close to the singular poses, the Jacobian matrices of the macro and macro–micro manipulator are well-conditioned and can be robustly used in the corresponding numerical computations.

5. Macro–Micro Optimal Trajectory Generation

Parallel macro–micro robots such as the one being investigated in this paper are kinematically redundant. In order to generate complete planar motion for the micro moving platform, generally only the micro or macro actuators are sufficient. However, in order to obtain very accurate positioning, a set of complete actuation levels is redundantly added to the manipulator design. Although the availability of the extra degrees of freedom can provide dexterous motion of the micro moving platform, proper utilization of this redundancy poses a challenging problem and several optimization techniques to solve this problem are reported in the literature, especially for serial manipulators. Redundant macro–micro manipulators have an infinite number of individual macro and micro motions that lead to the same final moving platform trajectory. This richness in the choice of individual motions complicates the manipulator control problem considerably. Typically, the kinematic component of a redundant macro–micro manipulator control scheme must generate a set of individual macro and micro manipulator trajectories, from the infinite set of possible trajectories, which causes the moving platform to follow a desired trajectory while satisfying additional constraints, such as collision avoidance, servomotor torque minimization, singularity avoidance or joint limit avoidance. Developing techniques to simultaneously achieve moving platform trajectory control while meeting additional task requirements is known as the redundancy resolution problem, since the motion of the manipulator joints must be resolved to satisfy both objectives. Since redundancy is an important evolutionary step toward versatile manipulation, research activity in redundancy resolution and related areas has grown considerably (e.g., Refs [23–25]). Most redundant manipulator control schemes resolve the redundancy through local or global optimization of various performance criteria. For the most part, researchers have focused on local optimization for redun-

dancy resolution by using the Jacobian pseudo-inverse to solve the instantaneous relationship between the joint and moving platform velocities. Redundancy resolution based on the Jacobian pseudo-inverse was first proposed by Whitney [26] and the null-space projection improvement was later proposed by Liégeois [27]. Baillieul [28] developed a different approach for local optimization by extending the Jacobian matrix to include the optimality condition. Anderson and Angeles [29] proposed a position-based local optimization scheme by solving a non-linear minimization problem with end-effector constraints.

In general, for a parallel manipulator, if $\dot{\mathbf{x}}$ is the N-dimensional velocity vector of the manipulator moving platform Cartesian space variable and $\dot{\mathbf{q}}$ is the $n > N$-dimensional vector of the limbs joint space variables, by defining the relation through Jacobians $\mathbf{J}_x$ and $\mathbf{J}_{\mathcal{L}}$:

$$\mathbf{J}_x \cdot \dot{\mathbf{x}} = \mathbf{J}_{\mathcal{L}} \cdot \dot{\boldsymbol{\mathcal{L}}}. \tag{47}$$

Then, due to the redundancy there are infinitely many solutions to the joint space variables $\dot{\boldsymbol{\mathcal{L}}}$, which can be found analytically by:

$$\dot{\boldsymbol{\mathcal{L}}} = \mathbf{J}_{\mathcal{L}}^{\dagger}\mathbf{J}_x\dot{\mathbf{x}} + \big(I - \mathbf{J}_{\mathcal{L}}^{\dagger}\mathbf{J}_{\mathcal{L}}\big)\dot{\boldsymbol{\sigma}}, \tag{48}$$

in which the pseudo-inverse $\mathbf{J}_{\mathcal{L}}^{\dagger}$ is defined by:

$$\mathbf{J}_{\mathcal{L}}^{\dagger} = \mathbf{J}_{\mathcal{L}}^{\mathrm{T}}(\mathbf{J}_{\mathcal{L}}\mathbf{J}_{\mathcal{L}}^{\mathrm{T}})^{-1}. \tag{49}$$

In this solution $\dot{\boldsymbol{\sigma}}$ is an arbitrary limb velocity vector and $(I - \mathbf{J}_{\mathcal{L}}^{\dagger}\mathbf{J}_{\mathcal{L}})\dot{\boldsymbol{\sigma}}$ is its projection into the null space of $\mathbf{J}_{\mathcal{L}}$. The attractiveness of this approach is 2-fold. First, the pseudo-inverse is one of the types of generalized inverse that has a least-squares property, minimizing $\dot{\boldsymbol{\mathcal{L}}}^{\mathrm{T}}\dot{\boldsymbol{\mathcal{L}}}$. Presumably, any limb is prevented from moving too fast, leading to a more controllable motion. Second, the redundancy available beyond that required for the micro motion is succinctly characterized by the null space of the Jacobian, which may be freely utilized to assist in the realization of some chosen objective. Liégeois [27] developed a general formation that tends to minimize a position-dependent scalar performance criterion $V(\dot{\mathbf{q}})$, in which the nullspace vector $\dot{\boldsymbol{\sigma}} = \frac{\partial V}{\partial q}k$, where k is an arbitrary constant. By this means $\dot{\boldsymbol{\sigma}}$ projects the gradient of V onto the joint motion in such a way as to reduce V through subsequent motion:

$$\dot{\boldsymbol{\mathcal{L}}} = \mathbf{J}_{\mathcal{L}}^{\dagger}\mathbf{J}_x\dot{\mathbf{x}} + \big(I - \mathbf{J}_{\mathcal{L}}^{\dagger}\mathbf{J}_{\mathcal{L}}\big)\frac{\partial V}{\partial \mathcal{L}}k. \tag{50}$$

Yoshikawa [30] proposed maximizing a manipulatability measure w, given by:

$$w = \sqrt{\det(J^{\mathrm{T}}J)}. \tag{51}$$

Since at a singularity configuration $w = 0$, then by minimizing the scalar function $V = 1/w(\mathbf{q})$, the optimal solution tends to keep the manipulator configuration away from singularities. In the following subsections an analysis based on macro–micro Jacobian matrices is developed to design optimal trajectories for the macro and micro manipulator. Two scenarios are examined here in which in the first case minimal

relative motion for the micro manipulator is considered, while in the second case for some singular configurations the optimal trajectory is designed to maximize the manipulability measure of the macro–micro manipulator.

5.1. Micro Minimal Motion

Consider the accurately positioning problem of the feed in the LCM/CPM structural design of the LAR. For sufficient coverage of the sky, at the macro level the LCM must be capable of positioning the receiver for a wide range of zenith and azimuth angles. Once the receiver is in place, the micro level position control of the tethered aerostat system responds to disturbances such as wind gusts in order to limit the movement of the receiver to centimeter accuracy. Hence, the workspace of LCM is much larger than that of the CPM and at the micro level the manipulator must be able to respond to high-frequency oscillation induced by the wind gusts. Therefore, the problem of trajectory planning for this structure is naturally defined as following. Assume that the micro manipulator final desired motion $\mathbf{x}_{g_\mathrm{d}} = [x_{g_\mathrm{d}}, y_{g_\mathrm{d}}, \psi_\mathrm{d}]^\mathrm{T}$ is given, the desired trajectory of the macro manipulator $\mathbf{x}_{G_\mathrm{d}} = [x_{G_\mathrm{d}}, y_{G_\mathrm{d}}, \phi_\mathrm{d}]^\mathrm{T}$ must be generated such that the relative motion of the micro manipulator with respect to the macro manipulator in minimized. In order to define the optimization problem for this goal, rewrite the Jacobian relation given in (37) which relates the micro moving platform velocity $\dot{\mathbf{x}}$ to that of the macro velocity $\dot{\mathbf{X}}$ and the micro relative motion in joint space $\dot{\boldsymbol{\ell}}$:

$$\mathbf{J}_m \cdot \dot{\mathbf{x}} = \mathbf{J}_{M_m} \cdot \dot{\mathbf{X}} + \dot{\boldsymbol{\ell}}. \tag{52}$$

The problem of optimal trajectory planning is, hence, finding the optimal macro manipulator velocity $\dot{\mathbf{X}}$ from a given desired trajectory for the micro manipulator $\dot{\mathbf{x}}$ which minimizes the relative motion of the micro manipulator. This equation can be cast into two Jacobians $\mathbf{J}_x$ and $\mathbf{J}_\theta$ in the form of:

$$\mathbf{J}_x \cdot \dot{\mathbf{x}} = \mathbf{J}_\theta \cdot \dot{\boldsymbol{\theta}}, \tag{53}$$

in which

$$\mathbf{J}_x = \mathbf{J}_m; \qquad \mathbf{J}_\theta = \left[\, \mathbf{J}_{M_m} \;\middle|\; I_4 \,\right]; \qquad \dot{\boldsymbol{\theta}} = \begin{bmatrix} \dot{\mathbf{X}} \\ \dot{\boldsymbol{\ell}} \end{bmatrix}; \tag{54}$$

where $\mathbf{J}_m$ and $\mathbf{J}_{M_m}$ are defined in (35) and (36), respectively, and I_4 denotes a 4×4 identity matrix. The optimization vector $\boldsymbol{\theta}$ is a 7×1 vector composed of the macro manipulator velocity and the relative micro limb velocities, and the Jacobian $\mathbf{J}_\theta$ is a 4×7 matrix. Comparing the Jacobian relation in the parallel manipulator in (53) with that to (47), the optimal redundancy resolutions is:

$$\dot{\boldsymbol{\theta}}_\mathrm{d} = \mathbf{J}_\theta^\dagger \mathbf{J}_x \dot{\mathbf{x}}_\mathrm{d} + \left(I - \mathbf{J}_\theta^\dagger \mathbf{J}_\theta\right) \frac{\partial V}{\partial \theta} k, \tag{55}$$

in which $\mathbf{J}_\theta^\dagger$ is the pseudo-inverse of $\mathbf{J}_\theta$ defined in (49).

In order to generate minimum relative motion in the micro manipulator, the proposed cost function V penalizes the relative motion by the following relation, in which $\|\cdot\|$ denotes the two-norm:

$$V_{\text{mm}} = \|\mathbf{x}_{G_{\text{d}}}(t) - \mathbf{x}_{g_{\text{d}}}(t)\|^2 + \|\dot{\boldsymbol{\ell}}(t)\|^2. \tag{56}$$

In this cost function the relative motion of the micro manipulator is penalized in the first term and the micro limb length velocities are also included to penalize the micro manipulator relative velocities. This optimization problem can be solved analytically by (55) or by numerical counterparts. In order to extend the solution to incorporate more comprehensive cost functions, in this paper the problem has been solved numerically using the quadratic programming routine (fmincon function of Matlab) for a given trajectory. The macro manipulator optimal trajectory and the relative motion of the optimal micro manipulator are illustrated in Figs 9 and 15, respectively. As shown in Fig. 9, the absolute micro manipulator motion is not distinguishable from that in the micro manipulator and the relative motion of the micro manipulator is near zero. Figure 15 illustrates the relative motion of the micro manipulator with respect to that of the macro manipulator and it is seen that the micro manipulator relative motion is zero by 10^{-7} accuracy. This result reveals the important fact that as for as the minimization of the micro manipulator relative motion is concerned, the desired trajectory of the macro manipulator can be designed without the need for any optimization and it can be chosen as $\mathbf{x}_{G_{\text{d}}}(t) = \mathbf{x}_{g_{\text{d}}}(t)$. Although, as

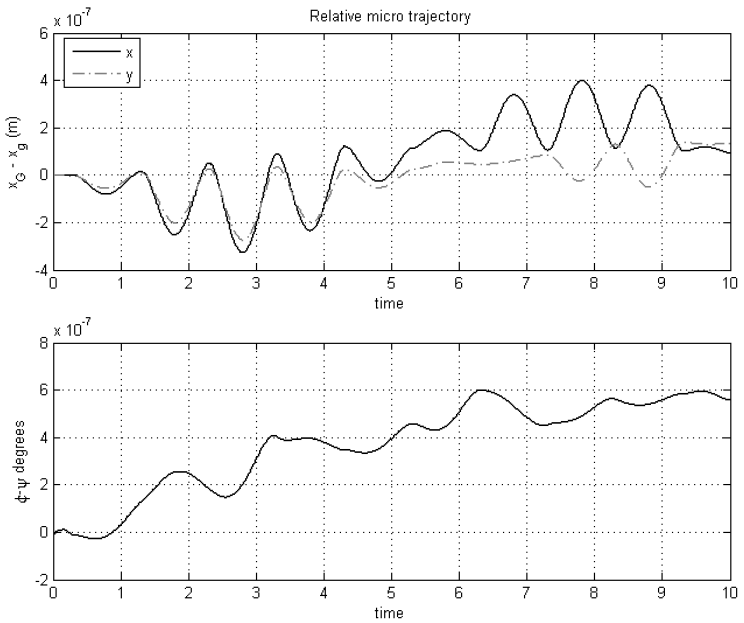

Figure 15. Optimal trajectory solution for micro minimal motion criteria: micro relative position and orientation.

reported in the next section, the optimization technique is used to incorporate other optimization purposes, the optimal solution obtained here confirms the expected trajectory by intuition.

5.2. Singularity Avoidance

Assume that the micro manipulator desired trajectory $\mathbf{x}_{g_\mathrm{d}} = [x_{g_\mathrm{d}}, y_{g_\mathrm{d}}, \psi_\mathrm{d}]^\mathrm{T}$ is given and the problem is to derive the desired trajectory of the macro manipulator $\mathbf{x}_{G_\mathrm{d}} = [x_{G_\mathrm{d}}, y_{G_\mathrm{d}}, \phi_\mathrm{d}]^\mathrm{T}$ in an optimal way to maximize the manipulability measure w defined in (51). It is evident that if the desired trajectory of the micro manipulator is far from the singularity configuration discussed in Section 4.3 the manipulability measure is well distributed for the entire trajectory and no special optimization is needed. Hence, in those cases the macro desired trajectory can be derived by the minimal micro motion trajectory described in Section 5.1. In order to show the effectiveness of the optimal trajectory planning though, consider a trajectory near the singular configuration of the manipulator as depicted in Fig. 16 by the dash-dotted line. In this trajectory no translational motion for the manipulator $x_{g_\mathrm{d}} = y_{g_\mathrm{d}} = 0$ is considered and, as is illustrated in Fig. 16 by the dash-dotted line, the orientation of the micro manipulator shows a sinusoid motion close to the singular configuration of the manipulator for the first 6 s and it is exactly at a singular configuration, $\psi = 90°$, for the remaining 4 s. The objective is to generate the macro manipulator motion such that the macro–micro manipulator tends away from the singular configuration, while the final micro manipulator trajectory follows exactly the desired motion.

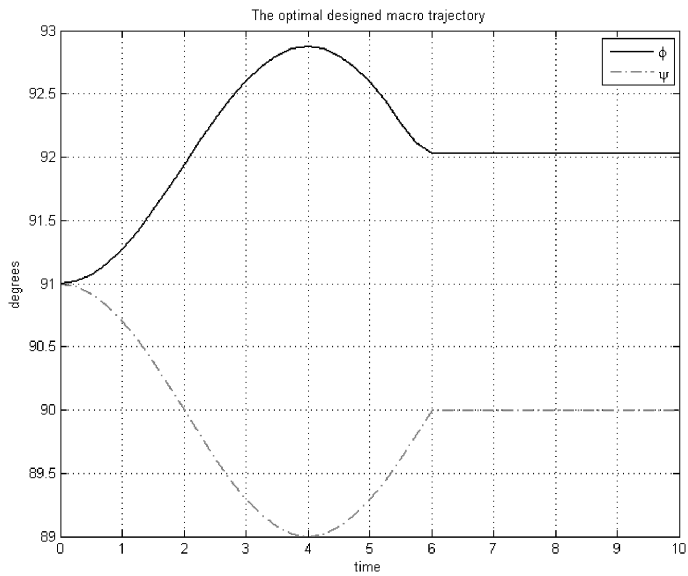

Figure 16. Optimal trajectory solution for singularity avoidance criteria: macro and micro absolute orientations.

The optimal problem is exactly as described in Section 5.1, while the cost function considered here to avoid singularity is:

$$V_{\mathrm{sa}} = \frac{1}{\sqrt{\det J_\theta^{\mathrm{T}} J_\theta}} + \kappa(V_{\mathrm{mm}}), \tag{57}$$

in which κ is a small constant and V_{mm} is the cost function for minimal micro motion as given in (56). As before, this optimization problem has been solved numerically for the given trajectory and $\kappa = 10^{-6}$, and the macro manipulator desired trajectory and the relative motion of the micro manipulator are illustrated in Figs 16 and 17, respectively. As shown in Fig. 16, although the micro manipulator motion is preserved to be very close to $\psi = 90^\circ$ as given, the macro manipulator orientation starts with the same value as that of the micro, but it departs from that quickly to avoid getting close to the singular configuration $\phi = 90^\circ$. Singularity avoidance is clearly illustrated in Fig. 17, in which the relative micro manipulator orientation $\phi - \psi$ is plotted. As seen in Fig. 17 although the micro manipulator trajectory tends to singularity, the self motion of the micro manipulator is such that the relative orientation is kept away from zero, where singularity occurs. Concluding from the results obtained in this section and the preceding section, it is observed that considering a weighted cost function of the above two objectives can be used for the general trajectory planning of the macro–micro manipulator even if the trajectories are away from singular configurations. Although if *a priori* information about the desired trajectory predicts that the manipulator is away from its singular configuration, then the intuitive solution of the minimal micro motion, i.e., $\mathbf{x}_{G_{\mathrm{d}}}(t) = \mathbf{x}_{g_{\mathrm{d}}}(t)$,

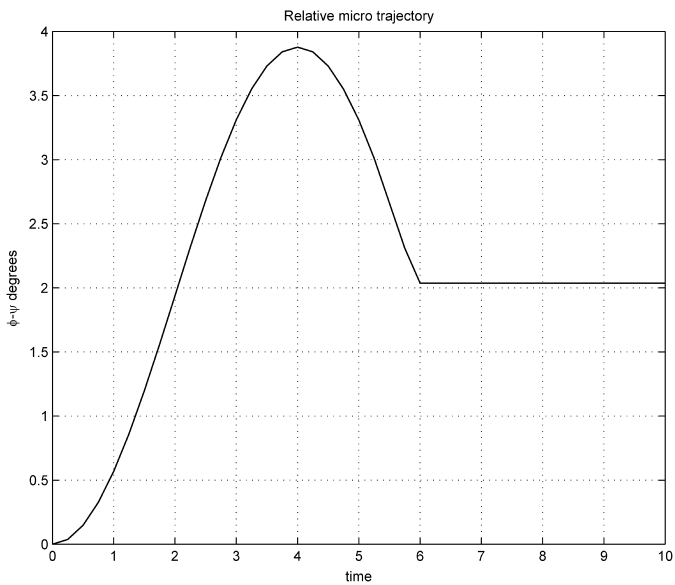

Figure 17. Optimal trajectory solution for singularity avoidance criteria: micro relative orientation.

can be used directly. However, in cases when such information is not available the weighted penalty function proposed in (57) with appropriate weighting selection can be used in the optimization technique.

6. Conclusions

In this paper the kinematic and Jacobian analysis of a macro–micro redundantly actuated parallel manipulator is studied in detail. The analyzed manipulator is a planar version adopted from the structure of the LAR, the Canadian design of the next generation of giant radio telescopes. In the LAR design the telescope receiver package is supported by a tension structure consisting of multiple long tethers and a helium-filled aerostat. The positioning structure of the receiver is designed as a macro–micro manipulator, in which at both the macro and micro levels two redundantly actuated cable-driven parallel manipulators are used and both manipulators experience 6-d.o.f. motion in space. The planar structure used in this paper is a simplified version of the LAR design in which the two important features of the main mechanism, i.e., macro–micro structure and actuator redundancy, are preserved in the planar structure. This structure is composed of two 3-d.o.f. parallel redundant manipulators at the macro and micro level, both actuated by cables. A thorough analysis on the kinematics and dynamics of the described macro–micro parallel manipulator has been developed and some closed-loop control topologies are proposed and simulated for this system. In this paper the kinematic and Jacobian analysis of this system is presented. It is shown that a unique closed-form solution to the inverse kinematic problem of such structure exists. Moreover, the forward kinematic solution is derived using numerical methods. Some simulations are presented for the macro–micro manipulators, by which the integrity and accuracy of numerical approaches used to derive the forward kinematic solution for this manipulator is presented. Furthermore, the Jacobian matrices of the manipulator at the macro and micro level are derived, and a thorough singularity and sensitivity analysis of the system is presented. It is shown that due to the crossed-cable structure used in the design the macro–micro manipulator has no singularity in the required workspace. Next, an optimal trajectory planning for the macro–micro manipulator is presented, in which the Jacobian matrices derived in the analysis are used in a quadratic programming approach to minimize performance indices like the minimal micro manipulator motion or singularity avoidance criterion. Minimal micro manipulator motion is preferable for LAR application, where due to the special design of the kinematic structure no singularity configurations are located within the manipulator workspace. However, for cases where the desired trajectories can become close to singularity configurations, the optimal trajectory planning with a weighted cost function is proposed to be used in practice.

Acknowledgements

The authors gratefully acknowledge the financial support received from the K. N. Toosi University of Technology, the Natural Sciences and Engineering Research Council of Canada and a PBEEE Quebec Visiting Scientist Award.

References

1. D. H. Chaubert, A. O. Boryssenko, A. van Ardenne, J. G. Bij de Vaate and C. Craeye, The Square Kilometer Array (SKA) antenna, in: *Proc. IEEE Int. Symp. Phased Array Systems and Technology*, Boston, MA, pp. 351–358 (2003).
2. M. V. Ivashina, A. van Ardenne, J. D. Bregman, J. G. B. de Vaate and M. van Veelen, Activities for the Square Kilometer Array (SKA) in Europe, in: *Proc. Int. Conf. Antenna Theory and Techniques*, Boston, MA, pp. 633–636 (2003).
3. B. Carlson, L. Bauwens, L. Belototski, E. Cannon, Y. Deng, P. Dewdney, J. Fitzsimmons, D. Halliday, K. Krschner, G. Lachapelle, D. Lo, P. Mousavi, M. Nahon, L. Shafai, S. Stiemer, R. Taylor and B. Veidt, The large adaptive reflector: a 200-m diameter, wideband, cm-wave radio telescope, in: *Radio Telescopes: Proc. SPIE Meeting 4015*, Bellingham, WA, pp. 33–44 (2000).
4. C. Lambert, A. Saunders, C. Crawford and M. Nahon, Design of a one-third scale multi-tethered aerostat system for precise positioning of a radio telescope receiver, in: *Proc. CASI Flight Mechanics and Operations Symp.*, Montreal, pp. 1–12 (2003).
5. C. Lambert, M. Nahon and D. Chalmers, Study of a multitethered aerostat system: experimental observations and model validation, *AIAA J. Aircraft.* **43**, 1182–1189 (2006).
6. L. Baron and J. Angeles, The direct kinematics of parallel manipulators under joint-sensor redundancy, *IEEE Trans. Robotics Automat.* **16**, 12–19 (2000).
7. X.-S. Gao, D. Lei, Q. Liao and G.-F. Zhang, Generalized Stewart–Gough platforms and their direct kinematics, *IEEE Trans. Robotics* **21**, 141–151 (2005).
8. G. Barrette and C. M. Gosselin, Determination of the dynamic workspace of cable-driven planar parallel mechanisms, *Trans. ASME J. Mech. Des.* **127**, 242–248 (2005).
9. S. Fang, D. Franitza, M. Torlo, F. Bekes and M. Hiller, Motion control of a tendon-based parallel manipulator using optimal tension distribution, *IEEE/ASME Trans. Mechatron.* **9**, 561–568 (2004).
10. J. P. Merlet, Direct kinematics of parallel manipulators, *IEEE Trans. Robotics Automat.* **9**, 842–846 (1993).
11. I. A. Bonev, J. Ryu, S.-G. Kim and S.-K. Lee, A closed-form solution to the direct kinematics of nearly general parallel manipulators with optimally located three linear extra sensors, *IEEE Trans. Robotics and Automat.* **18**, 148–156 (2001).
12. P. Ji and H. Wu, An efficient approach to the forward kinematics of a planar parallel manipulator with similar platforms, *IEEE Trans. Robotics Automat.* **18**, 647–649 (2002).
13. A. Fattah and G. Kasaei, Kinematics and dynamics of a parallel manipulator with a new architecture, *Robotica* **18**, 535–543 (2000).
14. B. Siciliano, The tricept robot: inverse kinematics, manipulability analysis and closed-loop direct kinematics algorithm, *Robotica* **17**, 437–445 (1999).
15. C. Gosselin and J. Angeles, Singularity analysis of closed-loop kinematic chains, *IEEE Trans. Robotics Automat.* **6**, 281–290 (1990).
16. J. Sefrioui and C. Gosselin, Singularity analysis and representation of planar parallel manipulators, *Robotics Autonomous Syst.* **10**, 209–224 (1992).

17. M. G. Mohamed and J. Duffy, A direct determination of the instantaneous kinematics of fully parallel robot manipulators, *ASME J. Mech. Transm. Automat. Des.* **107**, 226–229 (1985).
18. S. R. Oh, K. K. Mankala, S. K. Agrawal and J. S. Albus, Dynamic modeling and robust controller design of a two-stage parallel cable robot, *Multibody Syst. Dyn.* **13**, 385–399 (2005).
19. L. Yingjie, Z. Wenbai and R. Gexue, Motion control of a tendon-based parallel manipulator using optimal tension distribution, *IEEE Trans. Robotics* **22**, 198–202 (2006).
20. H. D. Taghirad and M. Nahon, Dynamic analysis of a macro–micro redundantly actuated parallel manipulator, *Adv. Robotics* **22**, in press (2008).
21. Y. X. Su, B. Y. Duan, R. D. Nan and B. Peng, Mechatronics design of stiffness enhancement of the feed supporting system for the square-kilometer array, *IEEE/ASME Trans. Mechatron.* **8**, 425–430 (2003).
22. G. Meunier, Control of an overactuated cable-driven parallel manipulator. *ME Thesis*, McGill University, Montréal (2006).
23. D. P. Martin, J. Baillieul and J. M. Hollerbach, Resolution of kinematic redundancy using optimization techniques, *IEEE Trans. Robotics Automat.* **5**, 529–533 (1989).
24. K. Glass, R. Colbaugh, D. Lim and H. Seraji, Real-time collision avoidance for redundant manipulators, *IEEE Trans. Robotics Automat.* **11**, 448–457 (1995).
25. Y. Nakamura and H. Hanafusa, Optimal redundancy control of robot manipulators, *Int. J. Robotics Res.* **6**, 32–42 (1987).
26. D. E. Whitney, Resolved motion rate control of manipulators and human prostheses, *IEEE Trans. Man Mach. Syst.* **MMS-10**, 47–53 (1969).
27. A. Liégeois, Automatic supervisory control of the configuration and behavior of multibody mechanisms, *IEEE Trans. Syst. Man. Cybern.* **SMC-7**, 868–871 (1977).
28. J. Baillieul, Kinematic programming alternatives for redundant manipulators, in: *Proc. IEEE Conf. Robotics and Automotion*, St Louis, MO, pp. 722–728 (1985).
29. K. Anderson and J. Angeles, Inematic inversion of robotic manipulators in the presence of redundancies, *Int. J. Robotics Res.* **8**, 80–97 (1989).
30. T. Yoshikawa, Analysis and control of robot manipulators with redundancy, in: *1st Int. Symp. on Robotics Research*, Bretton Woods, NH, pp. 735–348 (1984).

About the Authors

Hamid D. Taghirad received his BS degree in Mechanical Engineering from Sharif University of Technology, Tehran, Iran, in 1989, his MS in Mechanical Engineering, in 1993, and his PhD in Electrical Engineering in 1997, both from McGill University, Montreal, Canada. He is currently an Associate Professor with the Electrical Engineering Department and the Director of the Office of International Scientific Cooperation at K. N. Toosi University of Technology, Tehran, Iran. He became a member of IEEE in 1995, and his publications include two books, and more than 100 papers in international journals and conference proceedings. His research interests are robust and non-linear control applied to the robotic systems.

Meyer A. Nahon received the BS degree in Mechanical Engineering from Queens University, Kingston, Canada, the MS degree in Aerospace Engineering from the University of Toronto, Toronto, and the PhD degree in Mechanical Engineering from McGill University, Montreal, Canada. He was an Assistant and Associate Professor of Mechanical Engineering with the University of Victoria, Victoria, Canada, from 1991 to 2001, and since then he has been an Associate Professor of Mechanical Engineering at McGill University. His present research deals with various aspects of robotics, including dynamics and control of aerial and undersea vehicles; mechanics of parallel mechanisms; and distance determination algorithms. He is an Associate Fellow of the AIAA and the Canadian Aeronautics and Space Institute (CASI). He has received awards from the AIAA and CASI for his work on flight simulator motion systems and space-based robotics.